Journal of Power Sources 196 (2011) 9906–9915

Contents lists available at ScienceDirect

Journal of Power Sources

journal homepage: www.elsevier.com/locate/jpowsour

Degradation of polymer electrolyte membrane fuel cells repetitively exposed to reverse current condition under different temperature

Yoo Yeon Jo [a], EunAe Cho [b,*], Jung Hyeun Kim [a], Tae-Hoon Lim [b], In-Hwan Oh [b], Soo-Kil Kim [b], Hyung-Juhn Kim [b], Jong Hyun Jang [b]

[a] Department of Chemical Engineering, University of Seoul, 90 Junnong-dong, Dongdaemun-gu, Seoul 130-743, Republic of Korea
[b] Fuel Cell Center, Korea Institute of Science and Technology, 39-1 Hawolgok-dong, Sungbuk-gu, Seoul 136-791, Republic of Korea

ARTICLE INFO

Article history:
Received 15 April 2011
Received in revised form 27 June 2011
Accepted 5 August 2011
Available online 12 August 2011

Keywords:
Polymer electrolyte membrane fuel cells
Operating temperature
Startup/shutdown cycle
Carbon corrosion
Durability

ABSTRACT

Effects of operating temperature on performance degradation of polymer electrolyte membrane fuel cells (PEMFCs) were investigated under the repetitive startup/shutdown cycling operation that induced the so-called 'reverse current condition'. With repeating the startup/shutdown cycle, polarization curves, electrochemical impedance spectroscopy (EIS), cyclic voltammetry (CV), linear sweep voltammetry (LSV) were measured to examine in situ electrochemical degradation of the MEAs. To investigate physico-chemical degradation of the MEAs, scanning electron microscopy (SEM), electron probe micro analysis (EPMA), transmission electron microscopy (TEM) and Fourier transform infrared spectroscopy (FT-IR) were employed before and after the startup/shutdown cycling operation. With increasing operating temperature from 40 to 65 and 80 °C under the repetitive reverse-current condition, the cell performance decayed faster since corrosion of the carbon support and dissolution/migration/agglomeration of Pt catalyst were accelerated resulting in increases in ohmic and charge transfer resistance and loss of EAS.

1. Introduction

Polymer electrolyte membrane fuel cells (PEMFCs) have been paid attention as alternative power sources for automobile systems due to high power density and efficiency, rapid startup and low emission of side reaction products. For commercialization of PEMFCs, there are technical problems to be solved; cost and lifetime. For fuel cell vehicles, lifespan of 5000 h is required. However, current technology cannot achieve the target yet. In fuel cell vehicles, PEMFCs are exposed to dynamic operating conditions including load cycle, freeze/thaw cycle, variation in temperature and relative humidity and startup/shutdown cycle [1–3]. These dynamic conditions accelerate degradation of fuel cell components such as catalyst, support, membrane, gas diffusion layer, etc., resulting in irreversible degradation of cell performance. Particularly, startup/shutdown cycle is indispensable in operating fuel cell vehicles so that degradation of those fuel cell components is inevitable during startup/shutdown operation.

It has been reported that during startup/shutdown operation, membrane-electrode assemblies (MEAs) for PEMFCs degraded mainly by corrosion of carbon support and dissolution/migration/agglomeration of Pt catalyst of the cathode [4–7]. When a fuel cell vehicle is parked for a prolonged time, ambient air diffuses into the stacks since the cathode vent cannot be perfectly sealed and anode and cathode flow fields are eventually filled with air due to diffusion of air from cathode to anode through the membrane. If the fuel cell vehicle restarts under the condition with supplying hydrogen into the anode flow field, a H_2/air boundary is created in the anode flow field and high potential of 1.44 V [8] or twice of open circuit voltage (OCV) [9] is locally present on the cathode facing air in the anode flow field. The high potential that is locally induced on cathode under the so called 'reverse-current condition' can accelerate corrosion of carbon support dissolution/migration/agglomeration of Pt catalyst [4–11].

Operating conditions of PEMFCs such as relative humidity (RH) and stoichiometry of the reactant gases and cell temperature strongly affect the fuel cell performance and durability. With increasing operating temperature up to a certain degree, performance of PEMFCs generally improves primarily due to increases in catalytic activity and ionic conductivity of membrane. However, previous studies have shown that degradation of catalyst was accelerated at higher operating temperature [12,13] Bi and Fuller [12] investigated effects of temperature on durability of Pt/C catalyst with square-wave potential cycling and reported that degradation of the catalyst was faster in order of 80, 60, 40 °C. Lim et al. [13]

* Corresponding author. Tel.: +82 2 958 5279; fax: +82 2 958 5199.
E-mail address: eacho@kist.re.kr (E. Cho).

0378-7753/$ – see front matter © 2011 Elsevier B.V. All rights reserved.
doi:10.1016/j.jpowsour.2011.08.035

examined effects of operating conditions on carbon corrosion using on-line mass spectrometry. According to their results, emission of CO_2 caused by carbon corrosion increased with increasing the operating temperature and RH of reactant gases. In previous studies [4–7] we found that degradation of cathode exposed to the reverse current condition was accelerated at higher RH of the reactant gases since water facilitated corrosion of carbon support and oxidation of Pt catalyst. However, effects of cell temperature on performance degradation of PEMFCs repetitively exposed to the reverse current condition were little investigated.

In this study, we investigated effects of operating temperature on durability of PEMFCs under repetitive formation of the reverse current condition. To investigate in situ electrochemical degradation of membrane-electrode assemblies (MEAs), polarization curves, electrochemical impedance spectroscopy (EIS), cyclic voltammetry (CV) and linear sweep voltammetry (LSV) were measured before and after 200, 400, 600, and 1200 cycles. After 1200 startup/shutdown cycles, scanning electron microscopy (SEM), electron probe micro analysis (EPMA), transmission electron microscopy (TEM) and Fourier transform infrared spectroscopy (FT-IR) were carried out to examine physical and chemical degradation mechanisms of the MEAs.

2. Experimental

2.1. Preparation of a single cell

A single cell was assembled with a commercial MEA which has 25 cm^2 active area and 0.4 mg Pt/cm^2, graphite bipolar plates with serpentine flow pattern, gaskets, gas diffusion layers and endplates. After assembly, the single cell was activated at 0.42 V for 48 h. After the activation, cell temperature of single cell was controlled by a cartridge-type heater to be 40, 65 and 80 °C.

2.2. Startup/shutdown cycle

Fig. 1 shows a schematic voltage profile for the startup/shutdown cycle employed in this study. As an operating step, H_2 and air were supplied to a single cell for 17 s. Then, supply of air was stopped with connecting a dummy load between anode and cathode. In 10 s for the residual oxygen in cathode flow field to be exhausted, supply of H_2 was stopped. After 10 s, both flow fields of anode and cathode were purged with air for 20 s to simulate a prolonged parking condition. After the air purging step, H_2 was supplied to anode with disconnecting the dummy load and then in 3 s air was supplied to cathode. During the startup/shutdown cycle, gas flows were controlled by LabView software (National Instruments, Version 6.1), which controlled direction of 3-way solenoid valves. Flow rate of H_2 and air were 330 and 995 sccm, respectively, with relative humidity of 100%. The startup/shutdown cycling and electrochemical measurements were performed at cell temperatures of 40, 65 and 80 °C.

2.3. Electrochemical analyses

To examine electrochemical characteristics of single cells with the repetitive startup/shutdown cycles, polarization curves, electrochemical impedance spectroscopy (EIS), cyclic voltammetry (CV), linear sweep voltammetry (LSV) were measured before and after repeating 200, 600, 800 and 1200 cycles.

Polarization curves were measured using an electrical load (Daegil, ELT DC Electronic load ESL-300Z). Fully humidified H_2 and air passing through a bubbler-type humidifier were supplied to anode and cathode, respectively. Stoichiometric ration of H_2 and air were 1.5 and 2.0, respectively. EIS was performed with an IM6 model (Zahner) to obtain ohmic and charge transfer resistance. Fully humidified hydrogen and air were supplied for anode (counter/reference electrode) and cathode (working electrode). Voltage signal with a frequency range of 50 mHz–10 kHz and an excitation voltage of 5 mV were applied at a DC potential of 0.85 V. To calculate electrochemical active surface area (EAS), CV was performed with an IM6 model. A potential range was from 0.05 to 1.2 V at a scan rate of 0.05 V s^{-1}. To evaluate H_2 crossover current density, LSV was carried out in a potential range from 0.05 to 0.6 V at a scan rate of 1 mV s^{-1}. During the measurement of CV and LSV, fully humidified hydrogen and nitrogen were supplied to the anode and cathode, respectively [14].

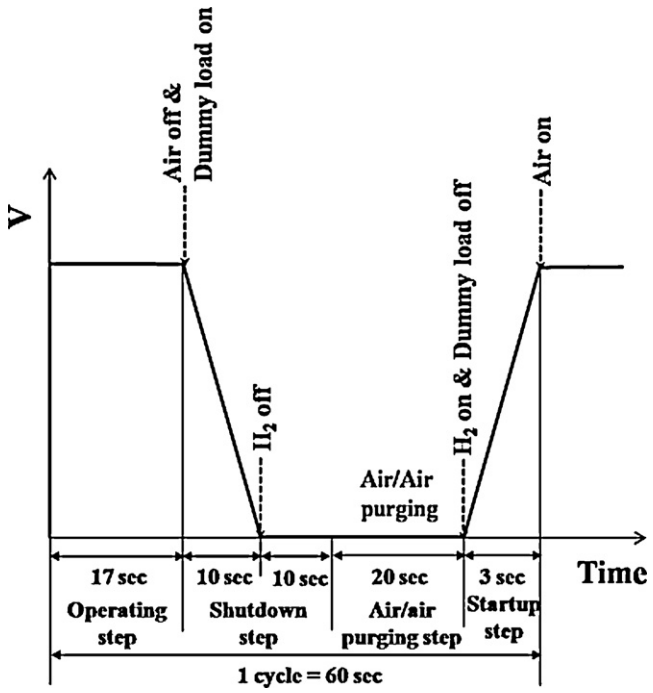

Fig. 1. A schematic voltage profile for the startup/shutdown cycle employed in this study.

2.4. Post-mortem analyses

To examine physical and chemical degradation mechanism of the MEAs, scanning electron microscopy (SEM), electron probe micro analysis (EPMA), X-ray diffraction (XRD), transmission electron microscopy (TEM) and Fourier transform infrared spectroscopy (FT-IR) were carried out for the MEAs before and after 1200 startup/shutdown cycling.

Thickness of electrodes and distribution of Pt catalysts were observed by SEM (XL-30 FEG) and EPMA (JXA-8500F) equipped with wavelength dispersive spectrometer (WDS). MEA samples were prepared in a form of small strip, which was cut in liquid nitrogen to get clear cross-sectional image.

FETEM was performed by TECNAI F30 at accelerating voltage of 200 kV to determine the average Pt particle size and distribution. The Pt catalysts were scrapped from the MEAs and dispersed in isopropyl alcohol (IPA) solvent using ultra sonication. A drop of the dispersion solution was placed onto a 200 mesh Cu grid, which was coated by carbon film using a micropipette. The Cu grid with the dispersion solution was dried in the oven at least 1 h to evaporate IPA solvent.

To examine chemical structure of membrane, FT-IR was performed by using Thermo Mattson Infinity gold FT-IR with an attenuated total reflectance (ATR) accessory. For sample preparation, MEAs were immersed in IPA solution for 20 min to remove

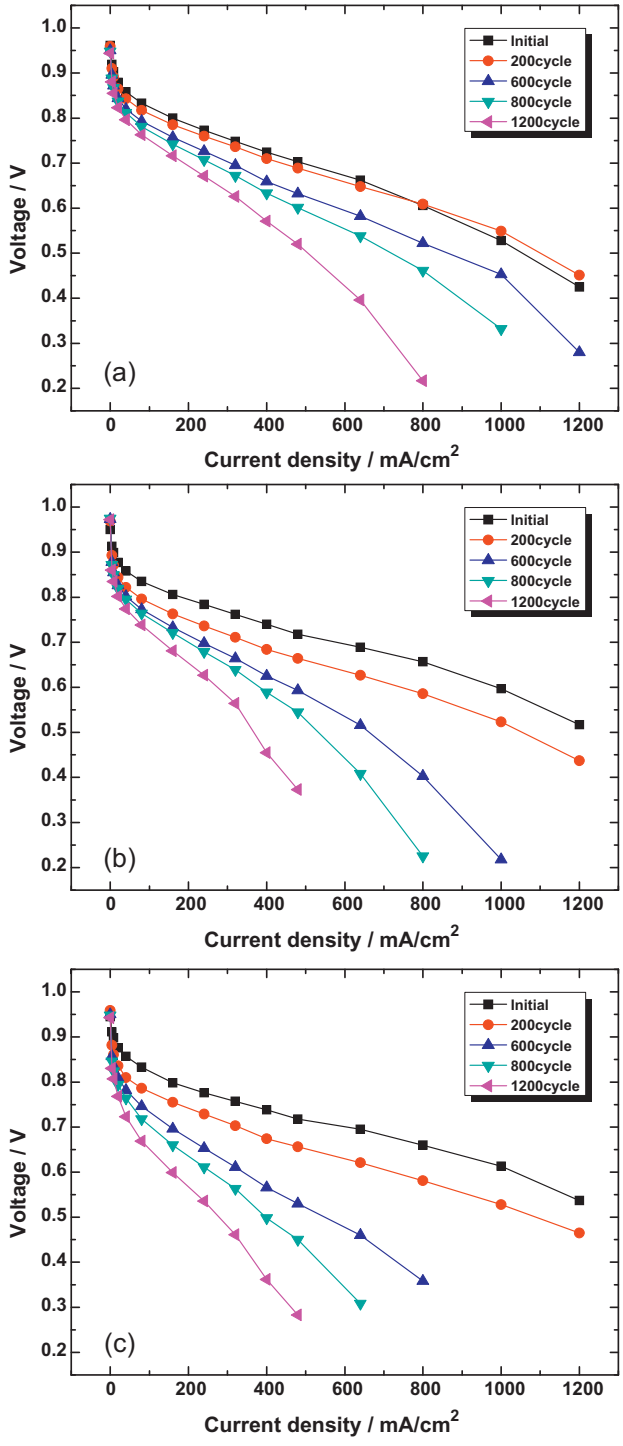

Fig. 2. *i–V* curves measured for the single cells before and after 200, 600, 800 and 1200 startup/shutdown cycles at operating temperatures of (a) 40, (b) 65, and (c) 80 °C.

anode and cathode from the membrane. The spectra were collected by an average of 36 scans in the range of 650–4000 cm^{-1}.

3. Results and discussion

3.1. Cell performance

Before and after 200, 600, 800 and 1200 startup/shutdown cycles, polarization curves were measured for a single cell, as shown in Fig. 2. At all operating temperatures, performance of the single cells lowered over the entire current density with increasing the number of startup/shutdown cycle, implying increases in activation, iR and concentration overpotential. Fig. 3(a) plots open circuit voltage (OCV) as a function of number of the cycle obtained from Fig. 2. OCV slightly changed during 1200 startup/shutdown cycles; 0.952 ± 0.007 V, 0.969 ± 0.007 V and 0.949 ± 0.006 V at the operating temperatures of 40, 65 and 80 °C, respectively. Since the variation in OCV is very small (less than 1% of the initial OCV value), it could be considered that gas crossover through the membrane was not remarkably affected by the repetitive formation reverse current condition. To estimate performance decay rate of the MEAs, cell voltage at 400 mA cm^{-2} was plotted in Fig. 3(b) from the data in Fig. 2. Initial cell voltage at 400 mA cm^{-2} was 0.72, 0.74 and 0.74 V at cell temperatures of 40, 65 and 80 °C, respectively. However, with repeating the startup/shutdown cycle, cell voltage at 400 mA cm^{-2} rapidly decreased in order of 80, 65 and 40 °C and, after 1200 cycles, lowered to 0.36, 0.46 and 0.57 V, respectively. Voltage decay rate at 400 mA cm^{-2} was calculated to be 0.13, 0.24 and 0.31 mV/cycle at 40, 65 and 80 °C, respectively. These results indicate that with increasing cell temperature from 40 to 80 °C, performance decay was clearly accelerated probably due to degradation of electrodes rather than membrane under the repetitive formation of the reverse current condition.

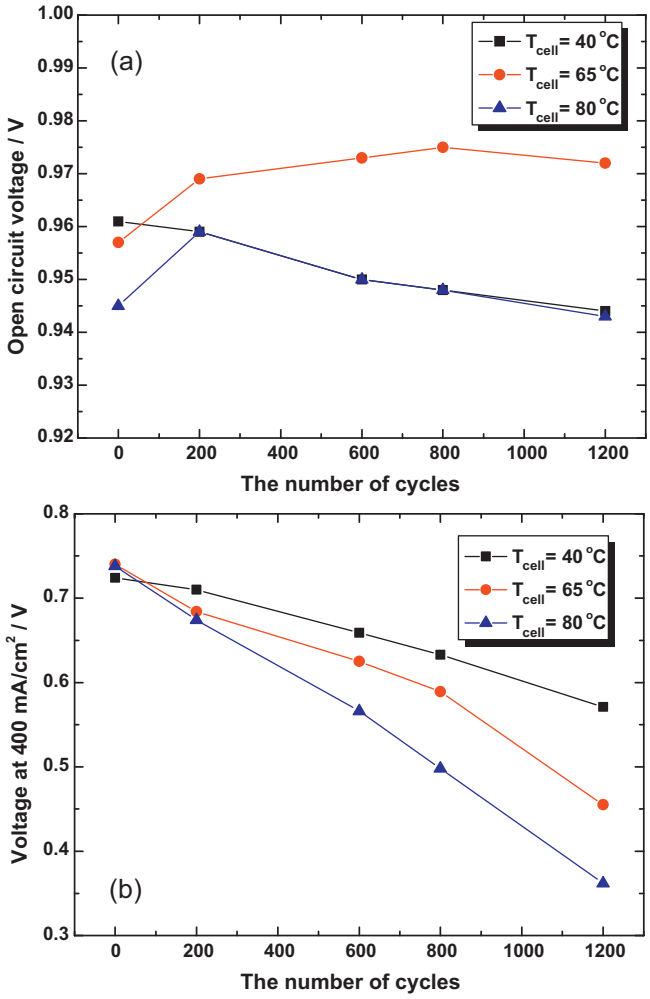

Fig. 3. Effects of operating temperature on (a) open circuit voltage (OCV) and (b) voltage at 400 mA cm^{-2}, obtained from the data in Fig. 2.

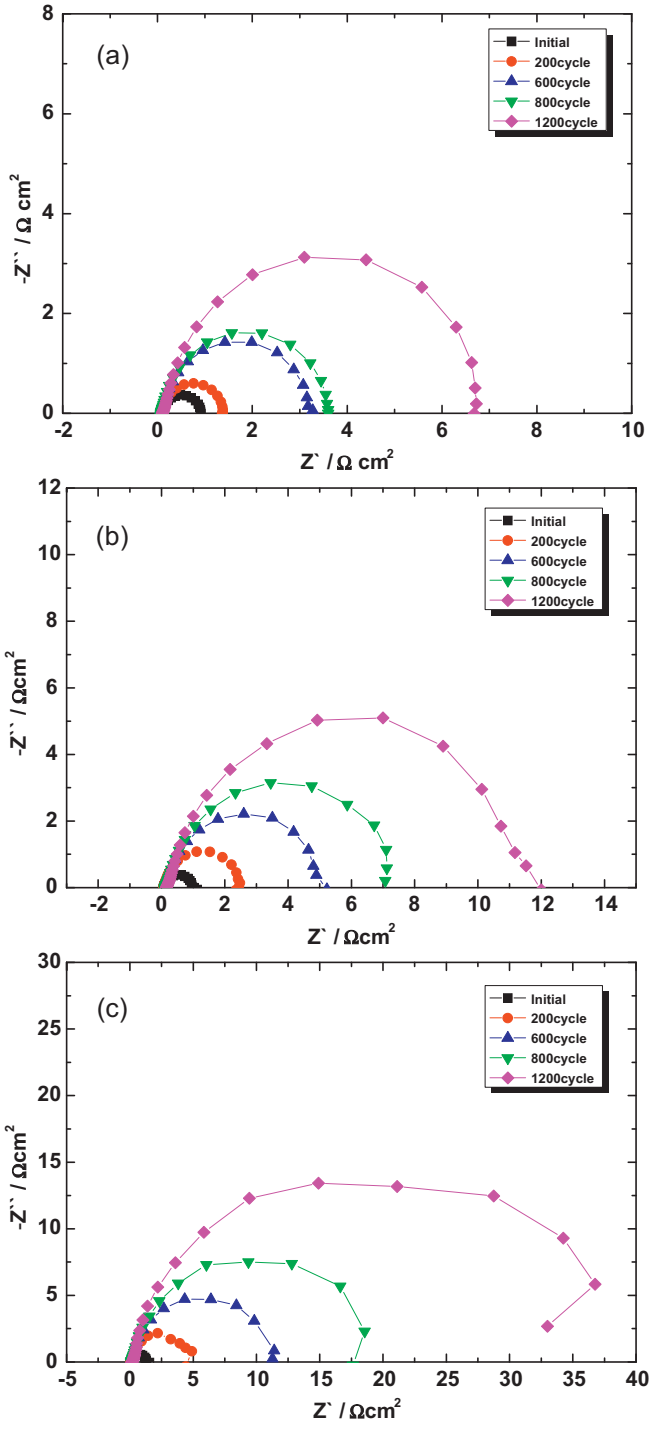

Fig. 4. Nyquist plots measured for the single cells before and after 200, 600, 800 and 1200 startup/shutdown cycles at operating temperatures of (a) 40, (b) 65, and (c) 80 °C.

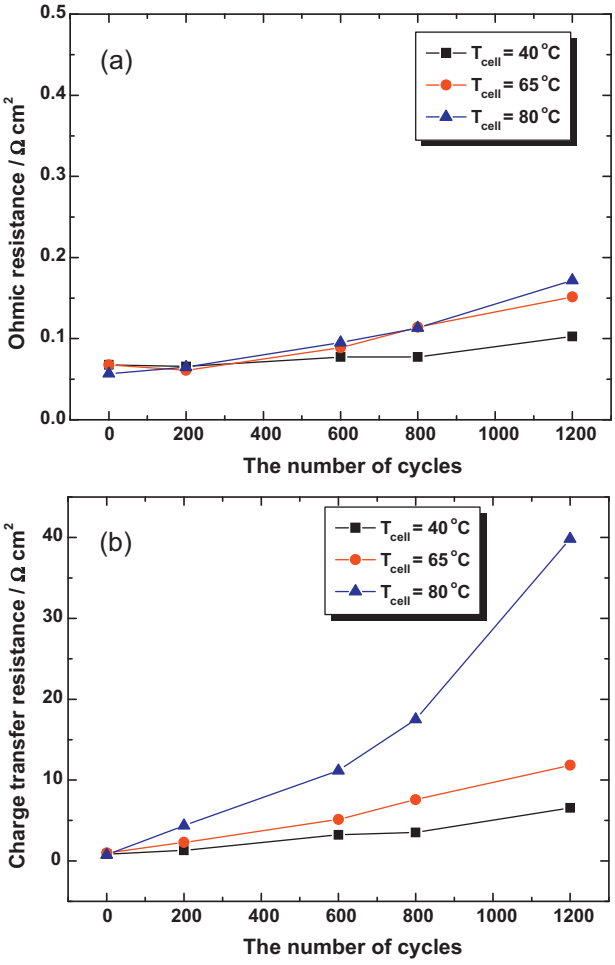

Fig. 5. Effects of operating temperature on (a) ohmic and (b) charge transfer resistance, obtained from the data in Fig. 4.

3.2. Electrochemical analyses

To examine influence of operating temperature on electrochemical degradation of single cell under the repetitive reverse current condition, EIS was carried out before and after 200, 600, 800 and 1200 cycles. Fig. 4 shows typical Nyquist plots for the single cells operated at 40, 65, and 80 °C. The ohmic and charge transfer resistance was measured by the *x*-axis intercept of high frequency (close to the origin) and diameter of a semi-circle, respectively [15] and summarized in Fig. 5. Both ohmic and charge transfer resistance increased with the cycling at different increment rate. During 1200 cycles at 40, 65 and 80 °C, ohmic resistance slightly increased from 0.068, 0.068 and 0.057 Ω cm^2 to 0.103, 0.152 and 0.172 Ω cm^2 while charge transfer resistance significantly increased from 0.841, 0.975 and 0.76 Ω cm^2 to 6.572, 11.849 and 39.828 Ω cm^2. In other word, ohmic and particularly charge transfer resistance increased much faster at higher operating temperature. Considering our previous results [4–7] at higher operating temperature, corrosion of carbon support and dissolution/migration/agglomeration of Pt catalyst could be accelerated and result in faster decay in the cathode, revealed by increase in ohmic and charge transfer resistance. The slight increase in ohmic resistance might be associated with degradation of the electrodes, i.e. decreases in electrical conductivity caused by loss of carbon support and Pt catalysts.

Cyclic voltammograms were measured before and after 200, 600, 800 and 1200 startup/shutdown cycles in order to estimate electrochemical active surface area (EAS, m^2 g^{-1} Pt), as shown in Fig. 6. The charging/discharging current of the double layer capacitor in the MEA, which was observed as current plateau at voltages of about 0.4–0.6 V, decreased more at higher operating temperature; i.e. current density at 0.5 V decreased from 3.27, 4.04 and 4.40 mA cm^{-2} to 2.92, 3.00 and 3.29 mA cm^{-2}, at cell temperature of 40, 65 and 80 °C, respectively. Decrease in the charging/discharging current of the double layer capacitor reflects that the interface between the electrode (cathode)

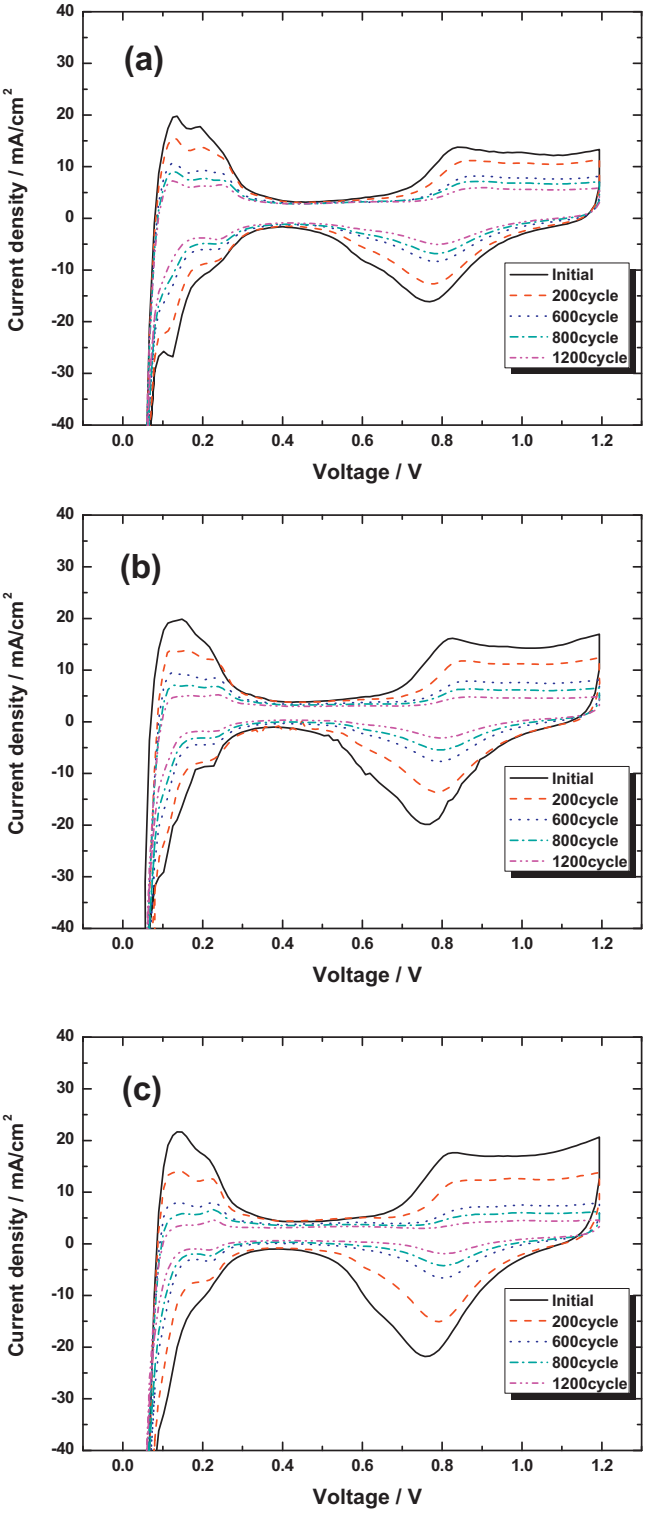

Fig. 6. Cyclic voltammograms measured for the single cells before and after 200, 600, 800 and 1200 startup/shutdown cycles at operating temperatures of (a) 40, (b) 65 and (c) 80 °C.

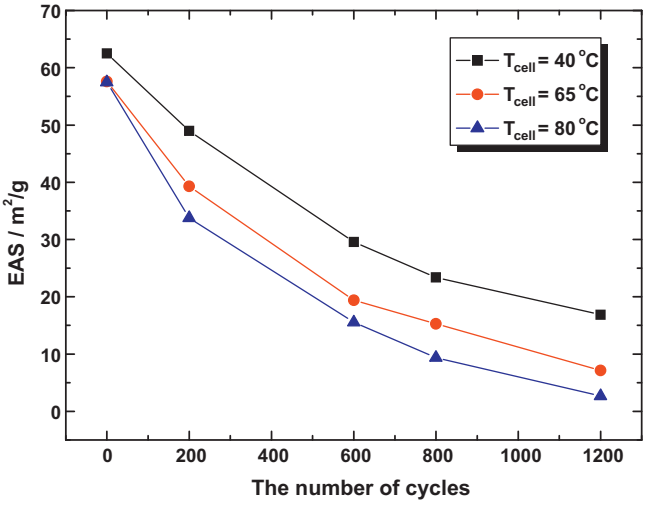

Fig. 7. Effects of operating temperature on electrochemical active surface area, calculated from the data in Fig. 6.

and electrolyte (membrane) was destroyed. Degradation of the cathode/membrane interface may be caused by carbon corrosion and/or dissolution/migration/agglomeration of Pt catalyst and/or decomposition of Nafion in the catalyst layer. More noticeable decrease in the charging/discharging current of the double layer capacitor at higher cell temperature could be related with severer degradation of the cathode/membrane interface as described above. These voltammograms clearly shows that hydrogen desorption peak observed at around 100 mV lowered with increasing number of the cycle, resulting in a reduction of EAS. EAS was calculated by the following equation:

$$\mathrm{EAS} = \frac{Q_{\mathrm{H}}}{[\mathrm{Pt}] \times 0.21}$$

where [Pt] represents the amount of Pt catalyst per unit area of the electrode, Q_{H} is the charge of hydrogen desorption, and 0.21 denotes the charge required to oxidize the hydrogen monolayer on bright Pt [16,17]. As presented in Fig. 7, during 1200 cycles, EAS decreased from initial value of 62.5, 57.6 and 57.46 $m^2\,g^{-1}$ to 16.84, 7.14 and 2.65 $m^2\,g^{-1}$ at 40, 65 and 80 °C, respectively. Clearly, reduction rate of EAS increased with increasing the cell temperature (0.038, 0.042 and 0.046 $m^2\,g^{-1}$/cycle; 0.061, 0.073 and 0.080%/cycle at 40, 65 and 80 °C, respectively). These results reflect that degradation of Pt catalyst in the cathode was severe in order of the operating temperature of 40, 65 and 80 °C.

To monitor hydrogen crossover through membrane, LSV was performed before and after 200, 600, 800 and 1200 cycles, as shown in Fig. 8. Hydrogen crossover current density measured at 0.4 V was plotted in Fig. 9. With increasing the cell temperature, hydrogen crossover current density increased, and, during 1200 startup/shutdown cycles, it remained almost constant; 1.124 ± 0.041, 1.68 ± 0.018 and 1.984 ± 0.055 mA cm^{-2} at 40, 65 and 80 °C. These results reflect that hydrogen crossover through the membrane was faster at higher operating temperature and that gas crossover through the membrane was not affected by repetitive 1200 startup/shutdown cycles.

3.3. Post-mortem analyses

Fig. 10 shows cross-sectional SEM and back-scattered SEM images taken before and after 1200 startup/shutdown cycling. MEA consisted of three layers; anode catalyst layer (top), electrolyte membrane (middle), and cathode catalyst layer (bottom). The catalyst layers were more clearly identified by BSEM images. During 1200 cycles, thickness of the anode catalyst layer was reduced from 12.7 μm to about 10 μm, irrespective of operating temperature and membrane thickness was kept almost constant to be about 20 μm. In contrast, thickness of the cathode catalyst layer was remarkably reduced from 13.68 μm to 9.52, 3.36 and 3.28 μm at cell

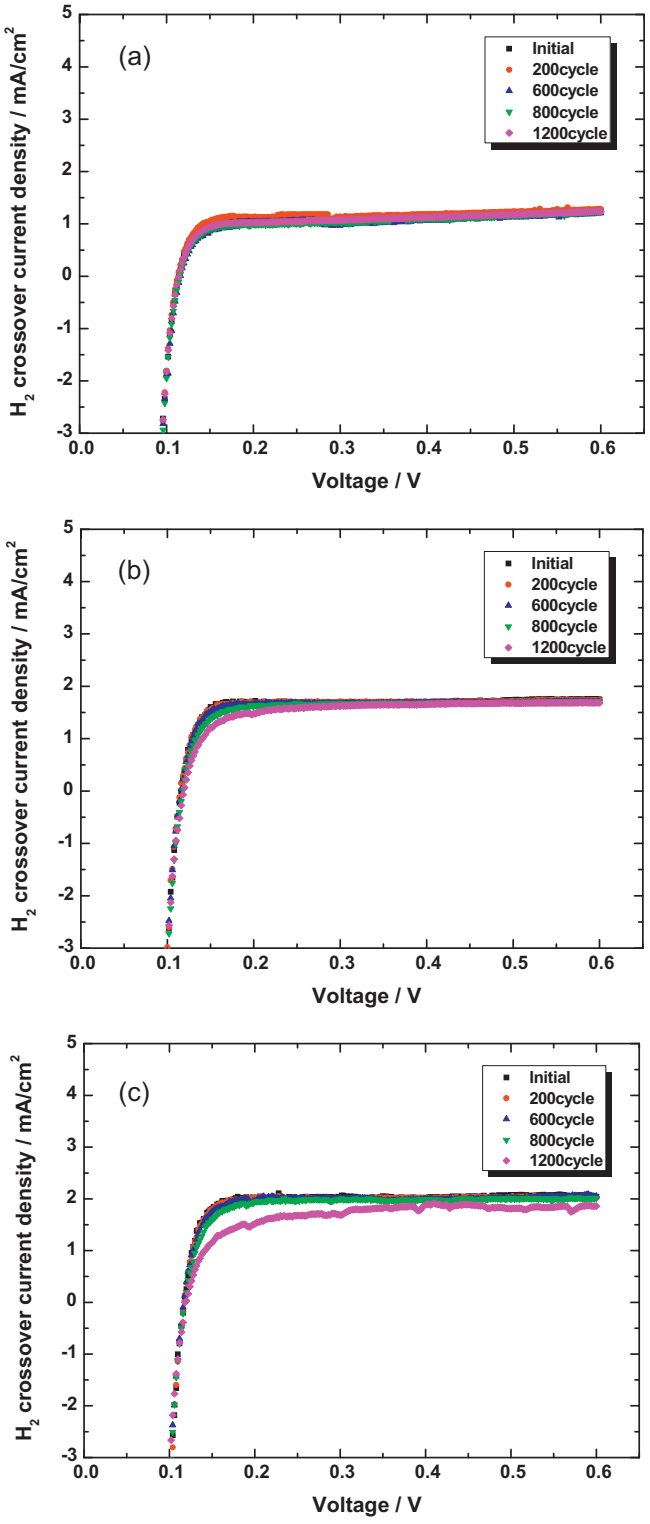

Fig. 8. Linear sweep voltammograms measured for the single cells before and after 200, 600, 800 and 1200 startup/shutdown cycles at operating temperatures of (a) 40, (b) 65 and (c) 80 °C.

temperatures of 40, 65 and 80 °C, respectively. These results show that the cathode catalyst layer was the most severely damaged by formation of the reverse current condition and the degradation rate significantly increased with operating temperature, in a good agreement with the above results. Faster decay of the cathode would be associated with higher corrosion rate of the carbon

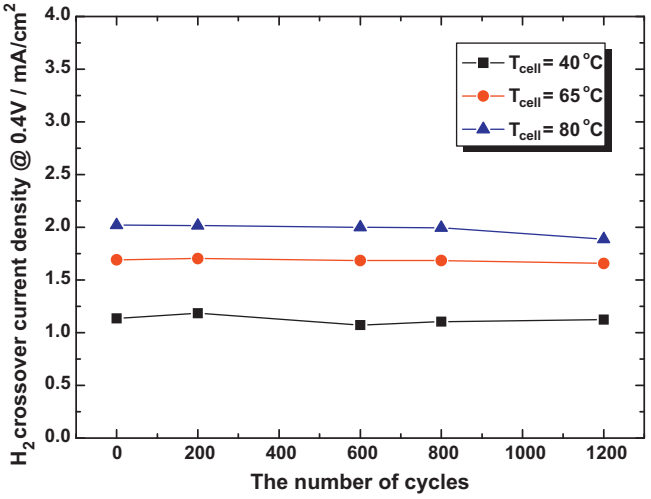

Fig. 9. Effects of the operating temperature on hydrogen crossover current density at 0.4 V, obtained from the data in Fig. 8.

support and facilitated dissolution/migration/agglomeration of Pt catalyst at higher operating temperature.

Fig. 11 shows Pt element mapping images for cross-sectional MEAs obtained by using EPMA before and after 1200 startup/shutdown cycles at 40, 65, 80 °C. The Pt elements of fresh MEA are well distributed in both electrodes. After 1200 cycles, thinning of the cathode and migration of cathode Pt into membrane was observed, particularly at higher operating temperature. At 80 °C, Pt band was clearly observed in the membrane. Therefore, it could be concluded the corrosion of the carbon support and dissolution and migration of Pt catalyst layer resulted in degradation of the cathode and hence cell performance.

FETEM images for Pt catalysts in both the anode and cathode before and after 1200 startup/shutdown operation are represented in Fig. 12. From the FETEM images, average particle size of Pt catalysts was measured and summarized in Table 1. The Pt catalysts of fresh MEA in both the anode and cathode seemed to be well-distributed and their average particle size was about 2.5 nm. During 1200 cycles, average Pt particle size of the anode increased to about 3.4 nm irrespective of operating temperature while that of the cathode increased to 3.67, 5.49 and 6.76 nm at operating temperatures of 40, 65 and 80 °C. These results exhibit that agglomeration of Pt catalyst was accelerated with increasing the operating temperature, which resulted in reduction of EAS and catalytic activity and hence in performance decay of PEMFCs.

Fig. 13 shows FT-IR spectra measured before and after 1200 startup/shutdown cycling to investigate effects of the startup/shutdown cycle on chemical structure of the membrane. During 1200 cycles, any peak shifts was not observed; C–F stretching at 980 cm^{-1}, S–O stretching at 1060 cm^{-1}, CF_2 symmetric stretching at 1100 cm^{-1}, and CF_2 asymmetric stretching at 1200 cm^{-1}. It could be concluded that degradation of the membrane was not a major factor in degrading performance of the single

Table 1
Average Pt particle size obtained from FETEM images in Fig. 12 for the anodes and cathodes of before and after 1200 startup/shutdown cycles at operating temperatures of 40, 65 and 80 °C.

Samples	Anode (nm)	Cathode (nm)
Before cycling	2.49	2.45
T_{cell} = 40 °C	3.41	3.67
T_{cell} = 65 °C	3.27	5.49
T_{cell} = 80 °C	3.36	6.76

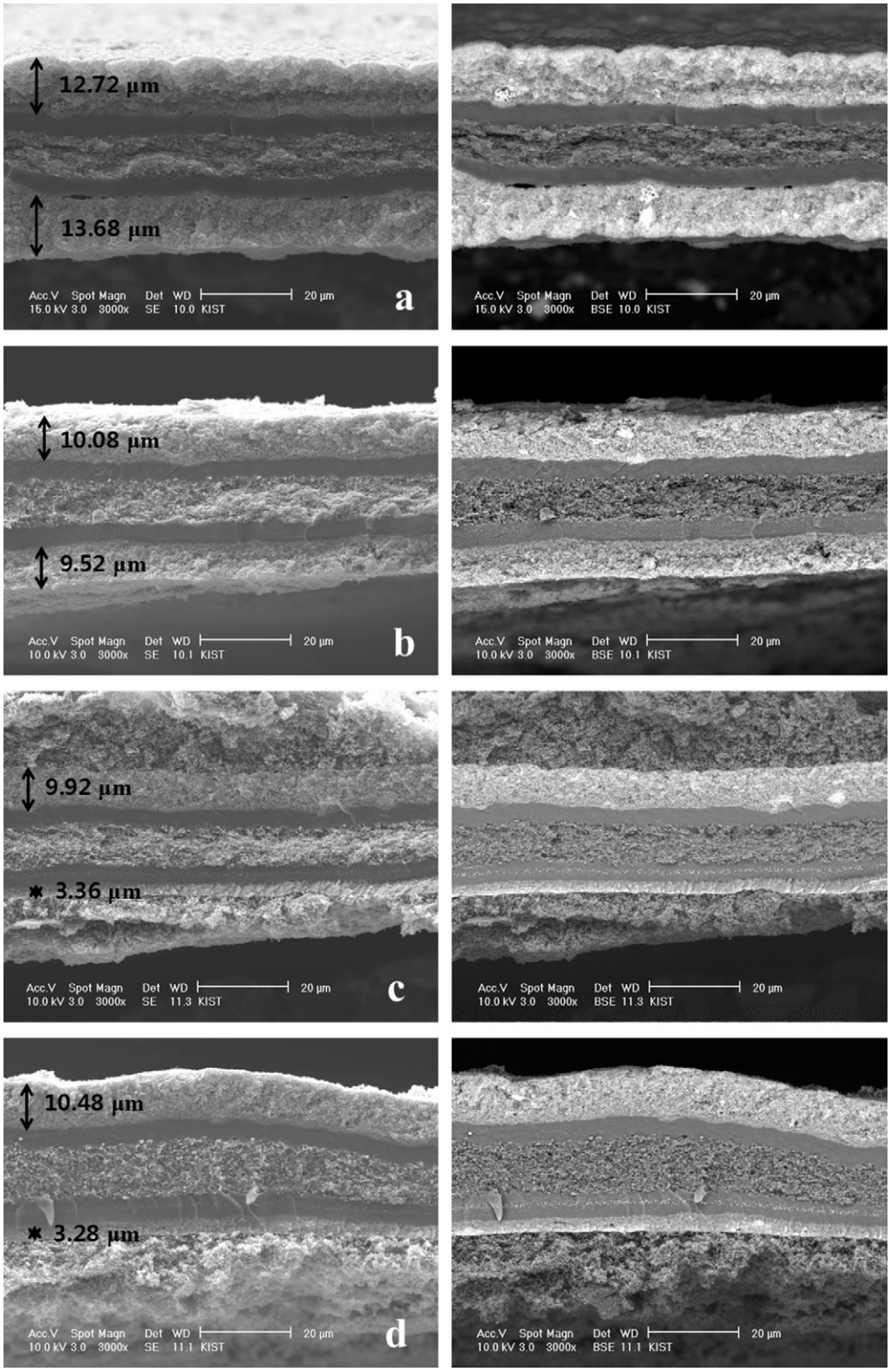

Fig. 10. Cross-sectional SEM (left) and BSE images (right) for the MEAs (a) before and after 1200 startup/shutdown cycles at operating temperatures of (b) 40, (c) 65 and (d) 80 °C.

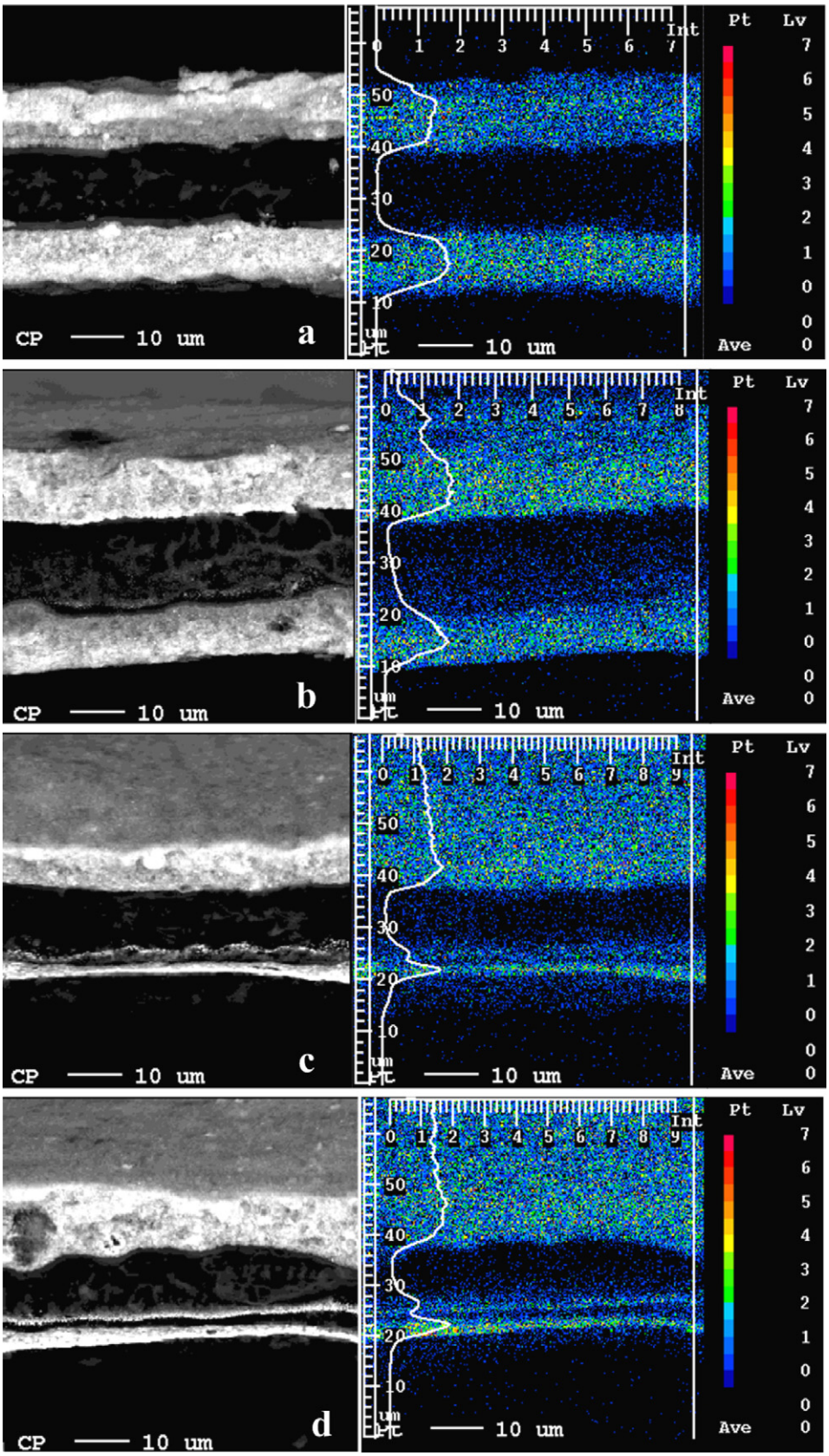

Fig. 11. Cross-sectional Pt mapping images for the MEAs (a) before and after 1200 startup/shutdown cycles at operating temperatures of (b) 40, (c) 65 and (c) 80 °C.

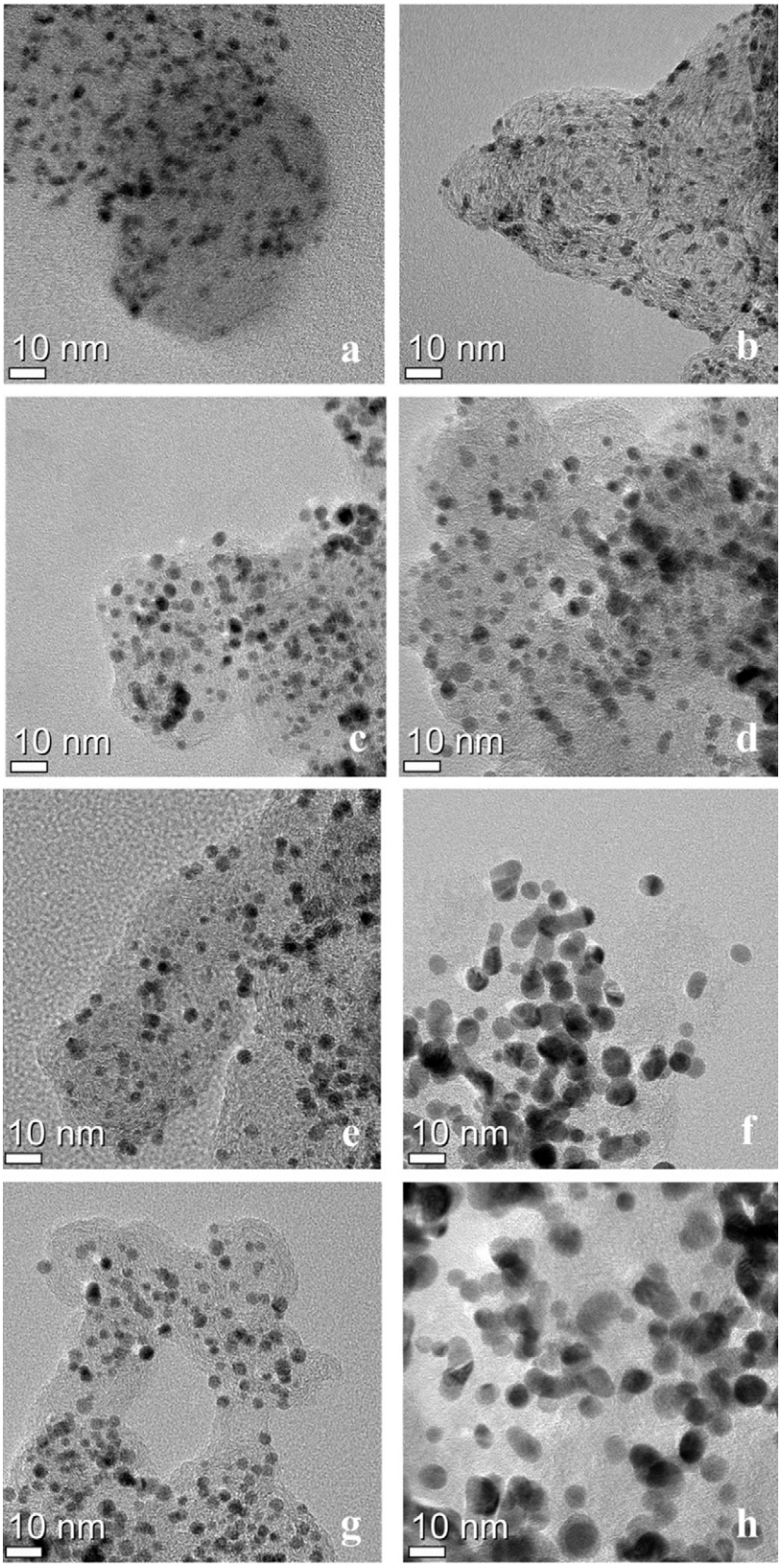

Fig. 12. TEM images measured for the anodes (left) and cathodes (right) of for the MEAs (a) and (b) before and after 1200 startup/shutdown cycles at operating temperature of (c) and (d) 40, (e) and (f) 65 and (g) and (h) 80 °C.

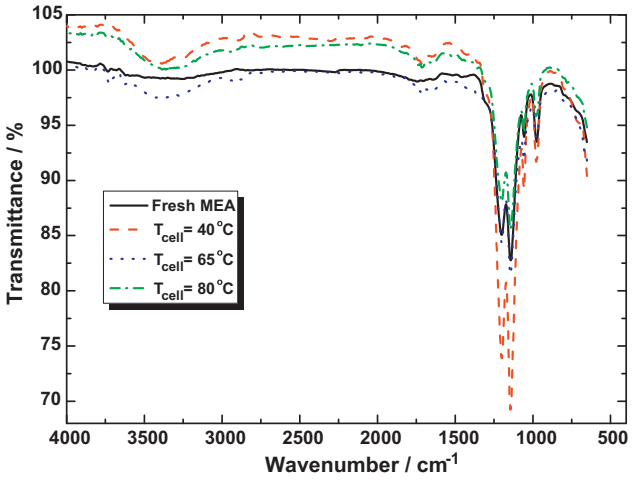

Fig. 13. FT-IR spectra measured for the membranes before and after 1200 startup/shutdown cycles at operating temperatures of 40, 65 and 80 °C.

cell exposed to the reverse current condition, in accordance with the above results that OCV and gas crossover current density was hardly affected by the startup/shutdown cycle.

4. Conclusions

In this study, effects of the operating temperature on performance degradation of PEMFCs exposed to repetitive formation of the reverse current condition were investigated at cell temperatures of 40, 65 and 80 °C. To evaluate electro- and physico-chemical characterization, various electrochemical analyses and post-mortem techniques were performed. With increasing operating temperature from 40 to 65 and 80 °C, corrosion of the carbon support and dissolution/migration/agglomeration of Pt catalyst were accelerated resulting in decay in cell performance as well as increases in ohmic and charge transfer resistance and loss of EAS.

Acknowledgements

This work was supported by New and Renewable Energy R&D Program and National R&D Organization for Hydrogen and Fuel Cell under the Korea Ministry of Knowledge Economy as a part of the development of mass production technology for low-cost PEMFC stacks.

References

[1] R. Borup, J. Meyers, B. Pivovar, Y.S. Kim, R. Mukundan, N. Garland, D. Myers, M. Wilson, F. Garzon, D. Wood, et al., Chem. Rev. 107 (2007) 3904–3951.
[2] F.A. de Bruijn, V.A.T. Dam, G.J.M. Janssen, Fuel Cells 8 (2008) 3–22.
[3] F. Rong, C. Huang, Z.S. Liu, D. Song, Q. Wang, J. Power Sources 175 (2008) 699–711.
[4] J.H. Kim, E.A. Cho, J.H. Jang, H.-J. Kim, T.-H. Lim, I.-H. Oh, J.J. Ko, S.C. Oh, J. Electrochem. Soc. 156 (2009) B955–B961.
[5] J.H. Kim, E.A. Cho, J.H. Jang, H.-J. Kim, T.-H. Lim, I.-H. Oh, J.J. Ko, S.C. Oh, J. Electrochem. Soc. 157 (2010) B104–B112.
[6] J.H. Kim, E.A. Cho, J.H. Jang, H.-J. Kim, T.-H. Lim, I.-H. Oh, J.J. Ko, I.-J. Son, J. Electrochem. Soc. 157 (2010) B118–B124.
[7] J.H. Kim, E.A. Cho, J.H. Jang, H.-J. Kim, T.-H. Lim, I.-H. Oh, J.J. Ko, I.-J. Son, J. Electrochem. Soc. 157 (2010) B633–B642.
[8] C.A. Reiser, L. Bregoli, T.W. Patterson, J.S. Yi, J.D. Yang, M.L. Perry, T.D. Jarvi, Electrochem. Solid-State Lett. 8 (2005) A273–A276.
[9] H. Tang, Z. Qi, M. Ramani, J.F. Elter, J. Power Sources 158 (2006) 1306–1312.
[10] T.W. Patterson, R.M. Darling, Electrochem. Solid-State Lett. 9 (2006) A183–A185.
[11] Z.Y. Liu, B.K. Brady, R.N. Carter, B. Litteer, M. Budinski, J.K. Hyun, D.A. Muller, J. Electrochem. Soc. 155 (2008) B979–B984.
[12] W. Bi, T.F. Fuller, J. Power Sources 178 (2008) 188–196.
[13] LimF K.H., H.-S. Oh, S.-E. Jang, Y.-J. Ko, H.-J. Kim, H. Kim, J. Power Sources 193 (2009) 575–579.
[14] T.E. Springer, T.A. Zawodzinski, M.S. Wilson, S. Gottesfeld, J. Electrochem. Soc. 143 (1996) 587–599.
[15] A.J. Bard, Electrochemical Methods, John Wiley & Sons, New York, 1980, p. 351.
[16] A.B. LaConti, M. Hamdan, R.C. McDonald, in: W. Vielstich, A. Lamm, H.A. Gasteiger (Eds.), Handbook of Fuel Cells: Fundamentals Technology and Applications, vol. 2, Wiley, New York, 2003, Chapter 21.
[17] S.S. Kocha, J.D. Yang, J.S. Yi, AIChE J. 52 (2006) 1916–1925.